

${}_{\Lambda\Lambda}^6\text{He}$ as a $\Lambda\Lambda$ Interaction Constraint

S. B. Carr and I. R. Afnan

*Department of Physics, Faculty of Science and Engineering, Flinders University of South
Australia, Bedford Park, SA 5042, Australia*

B. F. Gibson

*Theoretical Division, Los Alamos National Laboratory,
Los Alamos, NM 87545, USA*

(August 15, 2018)

Abstract

The Nijmegen OBE potential D is $SU(3)$ rotated to model the strangeness -2 sector of the baryon-baryon force. Soft core repulsion is introduced to regularize the singular nature of the OBE functions. The strength of the 1S_0 $t = 0$ interaction is adjusted to model three scenarios: (1) a bound state, (2) a narrow virtual, or antibound, state, and (3) an unbound state in which the force is weakly attractive. Using a separable approximation to these potentials, the binding energy of ${}_{\Lambda\Lambda}^6\text{He}$ is calculated in an $\Lambda\Lambda\alpha$ model. The resultant binding energies suggest that the strength of the 1S_0 $t = 0$ $\Lambda\Lambda$ and the nn interactions should be similar, if the coupling between the $\Lambda\Lambda$ and ΞN channels is taken into consideration.

21.80.+a, 21.30.-x, 21.10.Dr, 21.45+v

arXiv:nucl-th/9709003v1 4 Sep 1997

I. INTRODUCTION

The doubly strange $\Lambda\Lambda$ and Ξ hypernuclei provide the primary data that address the question of the properties of the $S = -2$ (strangeness -2) baryon-baryon interaction. Direct two-body scattering is impractical. In contrast, the data base for $S = 0$ NN scattering is relatively complete. Furthermore, although YN scattering data in the $S = -1$ sector are sparse, one does have differential and total cross section measurements to constrain theoretical models. Thus, there exists a keen interest in the reported $\Lambda\Lambda$ [1–4] and Ξ [5–10] hypernuclear events and in proposals to make new measurements at the Brookhaven AGS.

Our ultimate goal is to investigate the possibility of using the neutron spectrum from the $\Xi^- + d \rightarrow \Lambda + \Lambda + n$ reaction as a means to explore $\Lambda\Lambda$ scattering in the final state. The analogous proton spectrum from the low energy $n + d \rightarrow n + n + p$ reaction [11] exhibits a sizable final-state interaction peak which is governed by the nn scattering length and effective range. To carry out that investigation, we must first model the $\Lambda\Lambda$ – ΞN interaction using the available data on $\Lambda\Lambda$ and Ξ hypernuclei as constraints. The hypernucleus ${}_{\Lambda\Lambda}^6\text{He}$ becomes our laboratory for this purpose.

The single reported ${}_{\Lambda\Lambda}^6\text{He}$ event [2] is controversial [12]. However, the $\Lambda\Lambda$ separation energy

$$B_{\Lambda\Lambda} = B({}_{\Lambda\Lambda}^6\text{He}) - B({}^4\text{He}) \simeq 10.92 \pm 0.6\text{MeV} \quad (1)$$

yields a value for the $\Lambda\Lambda$ interaction matrix element

$$- \langle V_{\Lambda\Lambda} \rangle = B_{\Lambda\Lambda} - 2 \times B_{\Lambda}({}^5_{\Lambda}\text{He}) \simeq 4.7 \text{ MeV} , \quad (2)$$

which is consistent with the values of 4 – 5 MeV extracted from analysis of the heavier $\Lambda\Lambda$ hypernuclear events [1,3,4]. It is this $\Lambda\Lambda$ separation energy that serves to constrain the freedom in our modeling of the $\Lambda\Lambda$ – ΞN potential.

To minimize the number of parameters required in our strong interaction model, it is important to seek a unified model of the baryon-baryon force. In the one-boson-exchange (OBE) model approach [13–18], $SU(3)$ symmetry is assumed to hold at the level of coupling constants and vertices. (Alternative YN potential models have been produced by the Jülich group [19–22].) The $SU(3)$ symmetry is then broken by the use of physical masses for the baryons and mesons and by imposing phenomenological cutoff parameters to account for the short range properties of the forces. With no $S = -2$ scattering data, we employ an $SU(3)$ rotation from the $S = 0$ and $S = -1$ sectors to fix the $S = -2$ coupling constants. Only the short range cutoff parameters remain to be determined.

The $S \neq 0$ sector differs markedly in one aspect from the $S = 0$ sector. In the $S = 0$ sector one includes NN – ΔN coupling between the octet and decuplet implicitly in the OBE approach. However, the explicit inclusion of this coupling appears to play a relatively insignificant role in binding the ${}^3\text{H}$, ${}^3\text{He}$, and ${}^4\text{He}$ few-nucleon systems. In contrast, the ΛN – ΣN coupling of different octet members (the mass difference is ≈ 77 MeV) is a major feature of the $S = -1$ YN interaction, one which plays an important role in the obvious charge symmetry breaking exhibited by the $A = 4$ isodoublet [23–27] and the anomalously small binding of ${}^5_{\Lambda}\text{He}$ [23–25]. Therefore, one anticipates that the $\Lambda\Lambda$ – ΞN coupling of different octet members (the mass difference is only ≈ 25 MeV) may play an even larger role in the $S = -2$ sector.

The strong $nn\ ^1S_0$ interaction (almost bound system) has a possible $S = -2$ sector analog in the $\Lambda\Lambda-\Xi N$ interaction. That is, one might expect the $V_{\Lambda\Lambda}$ component of $V_{\Lambda\Lambda-\Xi N}$ to be a sizeable fraction of the strength of V_{nn} , if the $\{27\}$ is the dominant $SU(3)$ representation [28–30]; $\Lambda\Lambda-\Xi N$ coupling would then enhance the strength of the full $\Lambda\Lambda-\Xi N$ interaction, possibly to something comparable to that of the nn interaction. However, Hatrie-Fock investigations [31] imply that a $V_{\Lambda\Lambda}$ potential comparable in strength to that of the relatively weak $V_{\Lambda N}$ potential accounts for the binding energies of ${}_{\Lambda\Lambda}^6\text{He}$ and ${}_{\Lambda}^4\text{He}$. That is, one finds

$$\langle V_{\Lambda\Lambda} \rangle_{A=6} \simeq \langle V_{\Lambda N} \rangle_{A=4} \quad (3)$$

can account for the binding energy of both systems. A similar conclusion was reached by Bodmer *et al.* [32] and by Bandō [33].

This would-be discrepancy between a strong $V_{\Lambda\Lambda-\Xi N}$ potential and the relatively weaker extracted value of $\langle V_{\Lambda\Lambda} \rangle_{A=6}$ can be understood in terms of the probable suppression of $\Lambda\Lambda-\Xi N$ coupling in the $A = 6$ system. Just as the $\Lambda N-\Sigma N$ coupling appears to be suppressed in ${}_{\Lambda}^5\text{He}$ [34–39] (the conversion of the $t = 0$ Λ into a $t = 1$ Σ requires a corresponding transition from the $t = 0$ α core to an even-parity $t = 1$ excitation high in the α spectrum [31,39,40]), the $\Lambda\Lambda-\Xi N$ coupling is likely suppressed in ${}_{\Lambda\Lambda}^6\text{He}$, because converting an 1S_0 $\Lambda\Lambda$ pair into a similar ΞN pair will require either excitation of the α core or placement of the fifth nucleon in the ΞN^5 system in a $2s$ state in the shell model picture, due to the Pauli principle. Therefore, we argue that ${}_{\Lambda\Lambda}^6\text{He}$ probes primarily the diagonal element $V_{\Lambda\Lambda}$ of the $\Lambda\Lambda-\Xi N$ potential. (In contrast ${}_{\Lambda\Lambda}^4\text{H}$ would probe the full $\Lambda\Lambda-\Xi N$ coupling and ${}_{\Lambda\Lambda}^5\text{He}$ would strongly enhance the role of the $\Lambda\Lambda-\Xi N$ coupling because the ${}_{\Lambda}^4\text{He}-{}^4\text{He}$ binding energy difference would reduce dramatically the energy denominator in the transition. The ${}_{\Lambda\Lambda}^5\text{H}$ system was addressed as a three-body model by Myint and Akasishi [41].)

We report here bound-state calculations in which we test primary features of a series of two-body $\Lambda\Lambda-\Xi N$ separable potentials within the realm of a three-body $\Lambda\Lambda\alpha$ model of ${}_{\Lambda\Lambda}^6\text{He}$ [39]. We explore the effect of including explicit $\Lambda\Lambda-\Xi N$ coupling. In particular, we are able to find a model which produces an anti-bound state in the $\Lambda\Lambda-\Xi N$ system and also yields agreement with the experiment for $B_{\Lambda\Lambda}({}_{\Lambda\Lambda}^6\text{He})$. In addition, we examine models in which the $\Lambda\Lambda-\Xi N$ system is bound and in which it is weakly interacting. One would like to include the 0^+ excited state of the α particle in the calculation. However, given the paucity of physical observables available to constrain the $\Lambda\alpha$ (and therefore $\Lambda\alpha^*$) interaction, we must neglect any explicit $\Lambda\Lambda\alpha^*$ coupling effects in this investigation.

In the next section we discuss the parameterizations of the $\Lambda\Lambda$ and ΞN interactions which we use as input. In Sec. III we formulate the three-body bound-state model of ${}_{\Lambda\Lambda}^6\text{He}$. Our numerical results are summarized and briefly discussed in Sec. IV. Our conclusions are collected in Sec. V.

II. THE TWO-BODY INPUT: THE $\Lambda\Lambda$ AND ΞN INTERACTIONS

Ideally, to model the baryon-baryon (BB) interaction we need a description that is consistent with the underlying fundamental theory of the strong interaction, QCD, and yet at the same time provides a practical framework for calculations. An example of a QCD motivated model is the non-relativistic Quark Cluster Model (QCM) [42–44] which has been

applied extensively to the BB system [45–47]. While such models may give a good representation of the short range interaction, they are incapable of describing the longer range aspects of the potential. At intermediate to long distances a description of the potential in terms of physical baryons and mesons is expected to dominate. Thus for the NN force, the One-Pion-Exchange (OPE) tail is observed to be the main component of the force in this region. Extending this OPE potential to include heavier mesons that parameterize multi-pion exchanges, theorists since the sixties have constructed OBE models that account for the intermediate to long range components of the strong force. In this picture the short range component of the force is necessarily handled phenomenologically, either by the introduction of form factors for the meson-baryon vertices or by the introduction of short range cutoffs. The Nijmegen model D [14] is just such a OBE model, one which had as its prime motivation a description of all BB systems up to the pion production threshold within the same theoretical framework. This was achieved by invoking the internal symmetry $SU(3)_f$; that was assumed to be valid at the level of the baryon-baryon-meson coupling constants but to be dynamically broken by the inclusion of physical baryon and meson masses and by the inclusion of phenomenological short range cutoffs. We have extended the model to the $S = -2$ sector by performing an $SU(3)$ rotation for the coupling constants [30,48] and introducing a smooth short range cutoff to regularize the interaction as short distance.

A. OBE potentials in coordinate space

Starting from a Lagrangian picture, one can show that the basic OBE potential form will be a sum of terms involving central, spin-spin, tensor and more general terms involving the coupling of the spin and orbital angular momentum [13]. With the restriction to s-wave interactions only (*i.e.*, $\ell = 0$), these general terms disappear and the potential assumes the form

$$V_{\text{OBE}}(r) = V_c(r) + V_\sigma(r) \boldsymbol{\sigma}_1 \cdot \boldsymbol{\sigma}_2 + V_T(r) \mathbf{S}_{12}, \quad (4)$$

where

$$\mathbf{S}_{12} = 3 \boldsymbol{\sigma}_1 \cdot \hat{\mathbf{r}} \boldsymbol{\sigma}_2 \cdot \hat{\mathbf{r}} - \boldsymbol{\sigma}_1 \cdot \boldsymbol{\sigma}_2 \quad (5)$$

ouples $\ell = 0$ and $\ell = 2$ states for spin-triplet configurations. The two identical Λ hyperons must be in an antisymmetric state. Because the Λ carries isospin zero, and because we consider only s-wave two-body interactions, the only spin state allowed is the $s = 0$ configuration. This channel has no OPE component and consequently no tensor force, so that the term involving \mathbf{S}_{12} vanishes. The same is also true for the 1S_0 $t = 0$ and $t = 1$ ΞN channels. For the 3S_1 $t = 0$ and $t = 1$ ΞN channels, we can safely ignore the tensor force in a first calculation, due to the fact that $g_{\Xi\Xi\pi}$ is small [48] and it is the OPE potential that is primarily responsible for the tensor force component of the potential. Making this approximation for the 3S_1 ΞN interactions, our potentials take the form

$$V_{\text{OBE}}(r) = (V_c(r) + V_\sigma(r) \boldsymbol{\sigma}_1 \cdot \boldsymbol{\sigma}_2) \begin{pmatrix} 1 \\ \mathbf{t}_1 \cdot \mathbf{t}_2 \end{pmatrix}, \quad (6)$$

where we include the isospin factor $\mathbf{t}_1 \cdot \mathbf{t}_2$, for any isovector meson exchanges that contribute to $V_{\text{OBE}}(r)$. For the ΞN states of total isospin $t = 0, 1$ the isospin factor is normalized so that $\mathbf{t}_1 \cdot \mathbf{t}_2 = (-3, +1)$ respectively.

An important aspect of the $S = -2$ interaction is the coupling between the $\Lambda\Lambda$ and ΞN channels bearing the same quantum numbers. The $\Lambda\Lambda$ system has a threshold mass of $2m_\Lambda = 2231.2$ MeV, while the ΞN threshold lies only ~ 25 MeV above this value at $m_\Xi + m_N = 2257.01$ MeV. The proximity of these thresholds implies a need to include in the model a mechanism that allows for conversion between these two-particle states. Comparison of this system with the ΛN - ΣN system [49], where coupling is seen to play an important role in the determination of the binding energies of light Λ hypernuclei, supports this conjecture. It seems natural that the form of the OBE potential itself should provide this coupling through the exchange of strange mesons, namely the K and K^* . The Nijmegen scheme for achieving this is described briefly in the Appendix, where we detail the OBE potential in the $S = -2$ channel.

We must solve the Lippmann-Schwinger (LS) equation for the low energy scattering parameters for the relevant two-body systems. Rather than constructing the required potentials directly in momentum space, we first work in coordinate space where the physics is more transparent, and then we transform to momentum space. Until this point, we have not needed any phenomenology to specify the form of the interaction. The procedure we have adopted from the Nijmegen group is consistent and based on sound physical arguments, although to what extent $SU(3)$ is a valid symmetry [28,29] (at least for relating coupling constants) remains an open question. However, we must now resort to pure phenomenology, to the extent that we cannot determine the short range part (*i.e.*, $r < 0.5$ fm) of the interaction from a pure OBE description. Because we believe that the BB force is repulsive at short distances, we introduce a short range cutoff of the form $\mathcal{C} e^{-\mathcal{M}r}/(\mathcal{M}r)$. Here \mathcal{C} and \mathcal{M} (the cutoff mass) are free parameters that determine the size of the inner repulsion. The advantage of this procedure over introducing a hard core radius (r_c) cutoff is that we can quite easily transform this potential to momentum space, without having to integrate something that is infinite for $r < r_c$.

This prescription is somewhat analogous to Reid's [50] construction of his NN soft-core potential. However, we have not demanded the sophistication of Reid, for the lack of experimental data. We have freedom in choosing the parameters \mathcal{C} and \mathcal{M} ; actually \mathcal{M} can be fixed, leaving us with but one adjustable parameter. Therefore, we resort to analogy with other two-body systems, and to predicting binding energies and scattering observables of few-baryon systems, to determine the parameter \mathcal{C} , and thus to constrain the short range physics.

B. Soft-core potentials

If we examine the spin-isospin dependence of the $S = -2$ s-wave OBE potentials, we find that the $t = 0$ 1S_0 channel (*i.e.* the $\Lambda\Lambda$ - ΞN) is the most attractive. With essentially no experimental information at our disposal for the other ΞN channels, we have chosen to model their short range repulsion such that the overall potentials are weakly attractive, with effective range parameters $a \sim -1.75$ to -1.94 fm and $r \sim 3.0$ to 3.28 fm. The medium-to-long

range components of these potentials (*i.e.*, the OBE parts alone) are used as a guide as to which potential is the weakest and which the strongest.

The most interesting question to ask is how we should model the short range force in the $\Lambda\Lambda$ - ΞN system. We have already noted that the coupling between the $\Lambda\Lambda$ and ΞN channels is expected to play an important role. On the other hand, the uncertain short range physics will perhaps play no less a role once we have specified its form. With this in mind we have chosen a series of four soft-core potentials for the $\Lambda\Lambda$ - ΞN system, each with different two-body scattering properties. We construct model A to be weakly attractive, model B to support an antibound state in the $\Lambda\Lambda$ system and to be comparable in strength to the 1S_0 nn interaction, and two models which support $\Lambda\Lambda$ bound states, models C1 and C2. Model C1 supports a bound state of ~ 0.7 MeV, while model C2 supports a bound state of ~ 4.7 MeV. Both bound-state energies are measured with respect to the $\Lambda\Lambda$ threshold.

The potentials take the following basic form

$$V_{\xi}^{(i)}(r) = -V_0^{(i)} \left[\frac{e^{-m_i r}}{m_i r} - \mathcal{C} \left(\frac{\mathcal{M}}{m_i} \right) \frac{e^{-\mathcal{M}r}}{\mathcal{M}r} \right] \quad \xi = c, \sigma, \quad (7)$$

where m_i is the mass of the exchanged mesons (i). Here, $V_0^{(i)}$ symbolically represents the product of various coupling constants and mass factors that characterize the OBE potential form (see the Appendix). We choose to fix $\mathcal{M} = 2500$ MeV and vary \mathcal{C} to produce the required balance between inner range repulsion and outer range attraction, to construct potentials with the various two-body properties enumerated above. Depending on our choice for the parameter \mathcal{C} (see Table I) we generate potentials A, B, C1 and C2.

For some mesons the OBE contribution is repulsive, (*i.e.* $V_0^{(i)} < 0$ in Eq. (7)), and to guarantee that the cutoff is repulsive, we need to take $\mathcal{C} < 0$ for these mesons.

C. Momentum space potentials

In momentum space we construct the s-wave spin-isospin dependent potential as the $\ell = 0$ component of the partial wave expanded two-body potential

$$V_{\gamma\beta}(\mathbf{p}, \mathbf{p}') = \sum_{n,l,m_s,m_t} \langle \hat{p} | l n m_s m_t \rangle V_{\gamma\beta}^{nl}(p, p') \langle m_t m_s n l | \hat{p} \rangle, \quad (8)$$

where $n = \{s, t\}$ is the total spin and isospin of the two-body state. The subscripts γ and β label the two-body channels, *i.e.* $\gamma, \beta = (\Lambda \text{ or } \Xi)$. The s-wave momentum space potential, $V_{\gamma\beta}^{n0}(p, p') \equiv V_{\gamma\beta}^n(p, p')$, is now given in terms of the corresponding coordinate space potential by the Bessel transform

$$V_{\gamma\beta}^n(p, p') = \frac{2}{\pi} \int_0^\infty dr r^2 j_0(pr) V_{\gamma\beta}^n(r) j_0(p'r), \quad (9)$$

where we have chosen a δ -function normalization for the plane waves.

We interpret $V_{\gamma\beta}^n(r)$ as the sum of all the meson exchanges contributing to a given two-body state of definite total spin and isospin in coordinate space, with a similar meaning for $V_{\gamma\beta}^n(p, p')$. The explicit form for our soft-core potentials in momentum space for a given exchanged meson (i) is

$$V_{\xi}^{(i)}(p, p') = -\frac{V_0^{(i)}}{2\pi m_i p p'} \left[\ln \left(\frac{a+1}{a-1} \right) - \mathcal{C} \ln \left(\frac{b+1}{b-1} \right) \right], \quad \xi = c, \sigma, \quad (10)$$

where

$$a = \frac{m_i^2 + p^2 + p'^2}{2pp'} \quad \text{and} \quad b = \frac{\mathcal{M}^2 + p^2 + p'^2}{2pp'} \quad (11)$$

and \mathcal{C} and \mathcal{M} are the original parameters introduced in coordinate space. Explicit forms for the OBE potentials in p-space, for a given exchanged meson i , are obtained by replacing $\phi(m_i r)$ in the Appendix with

$$\phi(p, p'; m_i) = \frac{1}{2\pi m_i p p'} \left[\ln \left(\frac{a+1}{a-1} \right) - \mathcal{C} \ln \left(\frac{b+1}{b-1} \right) \right]. \quad (12)$$

D. Potential parameters

In momentum space, we can solve directly for the scattering amplitude (T -matrix) using standard K -matrix methods and Gauss-Legendre quadratures. The different thresholds coming from the rest mass difference between the $\Lambda\Lambda$ and the ΞN channels resides in the diagonal two-body Green's function

$$[\mathbf{G}_0]_{\gamma\beta} = \delta_{\gamma\beta} \left[E - M_{\gamma} - \frac{p^2}{2\mu_{\gamma}} \right]^{-1}, \quad (13)$$

where M_{γ} and μ_{γ} are the total and reduced mass in the channel γ .

The scattering length in a given channel a_{γ} and effective range parameter in that channel r_{γ} , for our potentials, are related to the diagonal elements of the T -matrix and the phase shifts by the relation [51]:

$$-\frac{1}{a_{\gamma}} + \frac{1}{2}p_{\gamma}^2 r_{\gamma} = p_{\gamma} \cot \delta_{\gamma} = -\frac{1 - i\pi\mu_{\gamma}p_{\gamma}T_{\gamma\gamma}}{\pi\mu_{\gamma}T_{\gamma\gamma}}. \quad (14)$$

In this case the scattering length and effective range for the ΞN channel are complex due to the presence of the other open channel, which is why the T -matrix $T_{\Xi\Xi}$ is not real at the ΞN threshold. These parameters, along with the two-body binding energies of soft core potentials C1 and C2, are presented in Tables II and III for each of our two-body interactions.

E. Separable potentials

As is well known, if we assume a separable form for the two-body potentials, then the analysis of the three-body problem is greatly simplified. For this reason we construct separable approximations to our soft-core potentials, by adjusting the parameters of the separable potentials to reproduce the scattering lengths and effective ranges shown in Tables II and III. This we do in each spin-isospin channel, and in the case of the $\Lambda\Lambda$ - ΞN $s = 0, t = 0$

channel we include the coupling phenomenologically by generalizing the form of our separable potential through the inclusion of the off-diagonal coupling strength $C_{\Lambda\Xi}$. Because we consider only s-wave interactions, our separable potentials take the form

$$V_{\gamma\beta}^n(p, p') = g_\gamma^n(p) C_{\gamma\beta}^m g_\beta^n(p'). \quad (15)$$

We choose Yamaguchi form factors [52]

$$g_\gamma^n(p) = (p^2 + \beta_\gamma^n)^{-1}, \quad (16)$$

which are given in terms of the range parameters β_γ^n . The sign of the coupling strength $C_{\Lambda\Xi}^n$ is determined by matching the sign of the $V_{\Lambda\Xi}$ matrix element for the separable potential with that of the soft-core potential.

For the single-channel potentials we can extract both the strength and range parameters using analytic expressions:

$$p_\gamma \cot \delta_\gamma = -\frac{\beta_\gamma}{2} \left(1 + \frac{2\beta_\gamma^3}{C_{\gamma\pi\mu_\gamma}} \right) + \frac{p_\gamma^2}{2\beta_\gamma} \left(1 - \frac{4\beta_\gamma^3}{C_{\gamma\pi\mu_\gamma}} \right) = -\frac{1}{a_\gamma} + \frac{1}{2} r_\gamma p_\gamma^2, \quad (17)$$

where γ is the channel label. In the case of the $\Lambda\Lambda$ - ΞN coupled-channels potentials, we determined the strength and range parameters by searching a five dimensional parameter space (for $C_{\Lambda\Lambda}$, $C_{\Lambda\Xi}$, $C_{\Xi N}$, β_Λ and β_Ξ) for the optimum χ^2 fit to the effective range parameters in both the $\Lambda\Lambda$ and ΞN channels. The calculations were performed for different values of momenta less than 0.1 fm^{-1} , to insure that the effective range parameters did not depend upon the choice of momenta.

The resulting separable potential parameters (*i.e.* the strength and range parameters) can be found in Tables IV and V. For comparison with the soft-core potential parameters, we also collect in Table VI the scattering lengths and effective ranges for the separable potentials in the $\Lambda\Lambda$ - ΞN coupled channel.

III. THE $\Lambda\Lambda\alpha$ THREE-BODY MODEL

The fact that ${}^4\text{He}$ is tightly bound suggests that we may model ${}^6_{\Lambda\Lambda}\text{He}$ as a $\Lambda\Lambda\alpha$ - $\Xi N\alpha$ system and thus neglect the possible excitation of the ${}^4\text{He}$ core. This puts some limitation on our model in terms of the role of the Pauli principle between the nucleon and the α in the $\Xi N\alpha$ channel, and therefore the role of the coupling between the $\Lambda\Lambda$ - ΞN coupled channels.

In a simple shell model, the α core may be considered as four nucleons in the $1s$ shell with total quantum numbers $J^\pi = 0^+$, $T = 0$. The Pauli principle will require that a fifth nucleon be placed in either the p or $s-d$ shell, with the latter being suppressed by the fact that it requires an additional $\hbar\omega$ in energy. In our three-body model this Pauli effect can be implemented by either requiring that the s -wave $N\alpha$ potential have its one Pauli forbidden bound state projected out, or by assuming that the s -wave interaction is repulsive, as has been done with success in bound-state calculations of ${}^6\text{Li}$ [53–55]. In the present investigation we use a repulsive $N\alpha$ s -wave potential.

The addition of the strangeness degree of freedom to this picture requires that we treat light hypernuclei as bound states of a nuclear core plus n hyperons. By treating the nucleon

and the hyperon as distinguishable baryons, we need not require that the hyperon and the nucleon core satisfy any Pauli principle. This makes the treatment of ${}^5_{\Lambda}\text{He}$ and ${}^6_{\Lambda\Lambda}\text{He}$ as $\Lambda\alpha$ and $\Lambda\Lambda\alpha$ bound states particularly attractive. In fact, we may use the experimental $\Lambda\alpha$ separation energy of $B_{\Lambda}({}^5_{\Lambda}\text{He}) \sim 3.1$ MeV to constrain our $\Lambda\alpha$ potentials.

A major feature of the $\Lambda\Lambda$ - ΞN interaction constructed in the previous section is the coupling between the $\Lambda\Lambda$ and ΞN channels in the 1S_0 , $t = 0$ partial wave. As noted above, one might expect the effective $\Lambda\Lambda$ matrix element in hypernuclei (*i.e.* $-\langle V_{\Lambda\Lambda} \rangle$) to be comparable to that of the nn interaction which is $-\langle V_{nn} \rangle \simeq 6 - 7$ MeV [56]. We argue that in ${}^6_{\Lambda\Lambda}\text{He}$ the coupling in a realistic $\Lambda\Lambda$ - ΞN free space interaction is strongly suppressed, because the conversion $\Lambda\Lambda \rightarrow \Xi N$ is Pauli blocked due to the fact that the fifth nucleon in $\Xi N\alpha$ should be in an antisymmetric state relative to the nucleons in the α particle. As a result, the diagonal $\Lambda\Lambda$ element of the interaction gives the major contribution to the binding energy. The Pauli blocking results in a reduced value of $-\langle V_{\Lambda\Lambda} \rangle \simeq 4 - 5$ MeV, in agreement with that extracted from the one experiment [2]. In other words, we anticipate that we can explain the ‘‘apparent’’ conflict between a realistic $\Lambda\Lambda$ - ΞN interaction and the anomalously small value for the extracted value of $-\langle V_{\Lambda\Lambda} \rangle$ in terms of the role played by $\Lambda\Lambda$ - ΞN coupling.

To test this hypothesis we performed bound-state calculations involving: (i) Only the $\Lambda\Lambda$ component of the amplitude due to the full $\Lambda\Lambda$ - ΞN force. (ii) The full $\Lambda\Lambda$ - ΞN interaction, which necessarily involves the introduction of the repulsive $S_{\frac{1}{2}} N\alpha$ potential to model the Pauli blocking, the p-wave αN interactions and an $\Xi\alpha$ potential. (iii) A single-channel effective $\Lambda\Lambda$ interaction designed to reproduce the scattering length and effective range parameters of the complete coupled-channel potential. We have already indicated why we believe (i) to be valid. Case (ii) provides a check on the effect of introducing a repulsive $S_{\frac{1}{2}} \alpha N$ interaction on the separation energy $B_{\Lambda\Lambda}({}_{\Lambda\Lambda-\Xi N}{}^6\text{He})$ of the hypernucleus involving a ΞN component in the wave function. Coupling between the three-body channels, $\Xi - (N\alpha)_{S_{\frac{1}{2}}}$ in a state of relative orbital angular momentum $\mathcal{L} = 0$, and $\Xi - (N\alpha)_{P_{\frac{1}{2}}}$ or $\Xi - (N\alpha)_{P_{\frac{3}{2}}}$ in a state of relative orbital angular momentum $\mathcal{L} = 1$, is allowed and satisfies parity and angular momentum conservation. Because the $P_{\frac{1}{2}}$ and the $P_{\frac{3}{2}}$ $N\alpha$ interactions are strong (both support resonances), we should include them in our bound-state calculation. If the above transitions between three-body channels are strong, then the existence of an excited ${}^6_{\Lambda\Lambda-\Xi N}\text{He}^*$ nucleus cannot be ruled out. Because the inclusion of these $N\alpha$ states (and also an $S_{\frac{1}{2}} \Xi\alpha$ interaction) is not beyond our computational capability, exploring the effect on the binding energy is worth the effort. However, the importance of these states involving p-wave αN interactions is limited on two accounts. Firstly, the system must couple to the ‘‘Pauli forbidden’’, $\Xi - (N\alpha)_{S_{\frac{1}{2}}}$ channel in a state of relative orbital angular momentum $\mathcal{L} = 0$, and secondly the probability for the transition between the three-body channels involving the $S_{\frac{1}{2}} N\alpha$ two-body cluster and the $P_{\frac{1}{2}}$ and $P_{\frac{3}{2}}$ $N\alpha$ two-body clusters should be small.

A. The $\Lambda\alpha$, $\Xi\alpha$, and $N\alpha$ potentials

There is little or no experimental data for the $\Lambda\alpha$ and $\Xi\alpha$ $S_{\frac{1}{2}}$ two-body systems. For the $\Lambda\alpha$ interaction there does exist as a constraint the experimental binding energy for the ground state of ${}^5_{\Lambda}\text{He}$. In that case we can also use our knowledge of the ΛN interaction and

construct an effective $\Lambda\alpha$ potential by folding the ΛN G -matrix [57–59] with the nucleon distribution for the ${}^4\text{He}$ core [60]. Any free parameter can then be adjusted to reproduce $B_\Lambda({}^5_\Lambda\text{He})$.

For the $\Lambda\alpha$ system, we take Yamamoto’s and Bandō’s effective YNG potential in coordinate space [60], which was designed to parameterize their ΛN G -matrix. In constructing this ΛN G -matrix for nuclear matter, they used the Nijmegen model D ΛN - ΣN coupled-channel potential as input. When applying this YNG potential to light hypernuclear systems such as ${}^5_\Lambda\text{He}$, they treated the Fermi momentum k_F as an adjustable parameter. We take $k_F = 0.932 \text{ fm}^{-1}$, so that our $\Lambda\alpha$ interaction has a bound state of $\sim 3.1 \text{ MeV}$ as observed experimentally. The central YNG potential has the form

$$V_{\Lambda N}^{t\ell s}(r; k_F) = \sum_{i=1}^3 w_i e^{-\left(\frac{r}{\beta_i}\right)^2} \quad (18)$$

with

$$w_i(k_F) = a_i + b_i k_F + c_i k_F^2, \quad (19)$$

where the parameters a_i , b_i , c_i , and the range parameter β_i , can be found in Table VII.

We are interested in the $t = 1/2$, $\ell = 0$, $s = 0$ and $s = 1$ channels, as the correct effective ΛN potential to be folded with the nucleon distribution of ${}^4\text{He}$ is a spin averaged sum of spin-triplet and spin-singlet interactions; *i.e.*,

$$V_{\Lambda N}^{eff}(r; k_F) = \frac{3}{4} V_{\Lambda N}^{\frac{1}{2}01}(r; k_F) + \frac{1}{4} V_{\Lambda N}^{\frac{1}{2}00}(r; k_F). \quad (20)$$

The $\Lambda\alpha$ potential is then given by

$$V_{\Lambda\alpha}(r) = \int d^3r' \rho_{{}^4\text{He}}(r') V_{\Lambda N}^{eff}(|\vec{r} - \vec{r}'|) \quad (21)$$

with

$$\rho_{{}^4\text{He}}(r') = \frac{4}{\pi^{\frac{3}{2}} b^3} e^{-\left(\frac{r'}{b}\right)^2}, \quad (22)$$

where $b^2 = \frac{2}{3}(r_{ch}^2 - r_p^2)$ and where $r_{ch} = 1.71$ and $r_p = 0.8 \text{ fm}$ are the charge radius of ${}^4\text{He}$ and the proton, respectively.

For comparison, we include the $\Lambda\alpha$ interaction of Kurihara *et al.* [61], which is parameterized as a two term Gaussian of the form

$$V_{\Lambda\alpha}(r) = V_R \exp[-(r/b_R)^2] - V_A \exp[-(r/b_A)^2], \quad (23)$$

where $V_R = 450.4 \text{ MeV}$, $V_A = 404.9 \text{ MeV}$, $b_R = 1.25 \text{ fm}$, and $b_A = 1.41 \text{ fm}$. This potential is referred to as the Isle potential [61]. It predicts a value for the (weak) lifetime of ${}^5_\Lambda\text{He}$ in good agreement with experiment, as well as reproducing the value for $B_\Lambda({}^5_\Lambda\text{He})$ of 3.1 MeV . In the absence of any data other than the Λ separation energy and the weak decay lifetime, it seemed prudent to restrict our consideration to these potential models rather than treat the $\Lambda\alpha$ effective range as a free parameter.

For the $\Xi\alpha$ system we have no experimental data at all. In this instance we make use of the bound-state data we have for other light Ξ hypernuclei [5,9,62,8], to construct a Ξ -nucleus potential that allows us to extrapolate to the $\Xi^5\text{He}$ system. In this approach we follow Dover and Gal [63]; we take their Ξ -nucleus potential and apply it to $\Xi^5\text{He}$. Their value for the Ξ -nucleus well depth is close to the theoretical prediction [48] for such a quantity, making use of Nijmegen model D for the ΞN interaction. The Ξ -nucleus potential, referred to as potential DG, has a Woods-Saxon form

$$V_{\Xi\alpha}(r) = -V_{0\Xi}(1 + e^{-(r-R)/a})^{-1}, \quad (24)$$

where $R = r_0 A^{\frac{1}{3}}$, $a = 0.65$ fm. We take $r_0 = 1.1$ fm, which in turn implies that $V_{0\Xi} = 24$ MeV. Here A is the mass number of the core nucleus under consideration, in our case $A = 4$.

We calculated the scattering length and effective range parameters for each of these potentials by transforming them to momentum space and solving the LS equation. The corresponding binding energies are listed along with the low energy scattering parameters in Table VIII. Separable approximations to these potentials (SYNG, SISle and SDG) were constructed. The parameters of these separable potentials were determined by demanding that the potentials reproduce the effective range parameters and binding energies given in Table VIII. These separable potentials have the same momentum space representation introduced previously in Eqs. (15) and (16) where $\gamma = \beta = Y\alpha$ with $Y = \Lambda$ or Ξ . The parameters of the potential $C_{Y\alpha}$ and $\beta_{Y\alpha}$ are determined from the effective range and scattering length through the following relations

$$\beta_i = \frac{3 \pm \sqrt{9 - 16\frac{r_i}{a_i}}}{r_i}; \quad C_i = \frac{4\beta_i^3}{\pi\mu_i(1 - \beta_i r_i)} \quad (25)$$

with $i = Y\alpha$ and $\mu_i = m_Y m_\alpha / (m_Y + m_\alpha)$.

Separable potentials exist in the literature for the $N\alpha$ interactions in the $S_{\frac{1}{2}}$, $P_{\frac{1}{2}}$ and $P_{\frac{3}{2}}$ channels. They have been used extensively in applications to α -d scattering and bound-state calculations (*e.g.*, ${}^6\text{Li}$ treated as an $NN\alpha$ system; see Ref. [55] and references cited therein). We utilize the parameters given in Ref. [55]; we consider model A for the p-wave interactions only. In momentum space these potentials assume the familiar form given in Eq. (15) with $\gamma = \beta = N\alpha$ and $n = \ell$, the relative orbital angular momentum. The form factors for the various $N\alpha$ channels are given by

$$g_{N\alpha}^\ell(p) = \frac{p^\ell}{[p^2 + \beta_{N\alpha}^{\ell^2}]^{(\ell+1)}}. \quad (26)$$

In this case the parameters were adjusted to fit the $N\alpha$ scattering data. The parameters of the $N\alpha$ potentials are given in Table IX.

B. The three-body equations

One of the most convenient forms of the Faddeev equations for practical solution of both the scattering and bound-state problems is the form in which Alt, Grassberger, and

Sandhas presented them, the AGS equations [64]. These equations appear in operator form as follows:

$$U_{\zeta\beta}(E) = \bar{\delta}_{\zeta\beta} G_0^{-1}(E) + \sum_{\gamma} \bar{\delta}_{\zeta\gamma} T_{\gamma}(E) G_0(E) U_{\gamma\beta}(E), \quad (27)$$

where $\bar{\delta}_{\zeta\beta} = 1 - \delta_{\zeta\beta}$, E is the total three-body energy, and $T_{\gamma}(E)$ is the two-body T -matrix for the interacting ($\zeta\beta$) pair in the three-body Hilbert space. The three-particle free Green's function has the form

$$G_0(E) = (E - H_0)^{-1}, \quad (28)$$

where H_0 , the Hamiltonian for the three non-interacting particles, is given by

$$H_0 = \sum_{j=1}^3 \left[m_j + \frac{k_j^2}{2m_j} \right] = \sum_{j=1}^3 m_j + \frac{p_{\zeta}^2}{2\mu_{\zeta}} + \frac{q_{\zeta}^2}{2\nu_{\zeta}}, \quad (29)$$

where the second equality holds in the three-body center of mass. We have included the rest masses in our definition of H_0 to allow for the correct incorporation of the different three particle thresholds when different mass eigenstates are coupled through the two-body transition amplitude T_{γ} [65]. Here \vec{p}_{ζ} stands for the momentum of the pair ($\beta\gamma$), while \vec{q}_{ζ} designates the momentum of the spectator ζ relative to the ($\beta\gamma$) pair. The Jacobi momenta and the reduced masses μ_{ζ} and ν_{ζ} are standard. The AGS operators, when sandwiched between the plane wave states $|\vec{q}_{\zeta}\vec{p}_{\zeta}\rangle$, represent the transition amplitudes for the process $\beta + (\gamma\zeta) \rightarrow \zeta + (\beta\gamma)$. Using standard three-body techniques, one can obtain equations for the physical transition amplitudes

$$X_{\zeta\beta} = \langle \phi_{\zeta} | G_0 U_{\zeta\beta} G_0 | \phi_{\beta} \rangle, \quad (30)$$

where $G_0|\phi_{\zeta}\rangle$ is the two-body state for the interacting pair ($\beta\gamma$). For two-body interactions of separable form, the AGS equations reduce to a standard set of coupled integral equation for the amplitudes $X_{\zeta\beta}$. Because our $\Lambda\Lambda\alpha$ has two identical Fermions, the two Λ s, we need to antisymmetrize the equations in return for a reduction in the number of coupled integral equations. This antisymmetrization has been detailed for the πNN [66] and YNN [65] systems to give a set of equations for the antisymmetric $\Lambda\Lambda\alpha$ amplitudes of the form

$$\begin{aligned} X_{\alpha\alpha} &= Z_{\alpha\Lambda} \tau_{\Lambda} X_{\Lambda\alpha} \\ X_{\Lambda\alpha} &= Z_{\Lambda\alpha} \tau_{\alpha} X_{\alpha\alpha} + Z_{\Lambda\Lambda} \tau_{\Lambda} X_{\Lambda\alpha}. \end{aligned} \quad (31)$$

If we label the two Λ s as 1 and 2, while the α as particle 3, the Born terms in Eq. (31) are given by

$$\begin{aligned} Z_{\alpha\Lambda} &= \sqrt{2} Z_{31}^c = \sqrt{2} \langle (12)3 | G_0 | (23)1 \rangle \\ Z_{\beta\zeta} &= Z_{\zeta\beta} \\ Z_{\Lambda\Lambda} &= -Z_{12} = -(-1)^R \langle (23)1 | G_0 | ((31)2) \rangle. \end{aligned} \quad (32)$$

Here the phase R results from the exchange of particles 3 and 1 in the ket [65].

These equations for the $\Lambda\Lambda\alpha$ system can be extended to include the coupling between $\Lambda\Lambda$ and ΞN two-body states, to encompass the contribution from the $\Xi N\alpha$ Hilbert space. Since we are only interested in the binding energy, we need to examine the spectrum of the kernel of the homogeneous equations, and in this case the initial state can be any of a number of possible two cluster states. To write an explicit form for our equation, we have assumed an initial state of $(\Lambda\Lambda)\alpha$. In this case our coupled homogeneous integral equations for the $\Lambda\Lambda\alpha$ - $\Xi N\alpha$ system take the form

$$\begin{pmatrix} X_{\alpha\alpha} \\ X_{\Lambda\alpha} \\ Y_{\alpha\alpha} \\ Y_{\Xi\alpha} \\ Y_{N\alpha} \end{pmatrix} = \begin{pmatrix} 0 & Z_{\alpha\Lambda}\tau_{\Lambda}^{\alpha\Lambda} & 0 & 0 & 0 \\ Z_{\Lambda\alpha}\tau_{\alpha}^{\Lambda\Lambda} & Z_{\Lambda\Lambda}\tau_{\Lambda}^{\alpha\Lambda} & Z_{\Lambda\alpha}\tau_{\alpha}^{\Lambda\Xi} & 0 & 0 \\ 0 & 0 & 0 & Z_{\alpha\Xi}\tau_{\Xi}^{\alpha N} & Z_{\alpha N}\tau_{N}^{\alpha\Xi} \\ Z_{\Xi\alpha}\tau_{\alpha}^{\Xi\Lambda} & 0 & Z_{\Xi\alpha}\tau_{\alpha}^{\Xi N} & 0 & Z_{\Xi N}\tau_{N}^{\alpha\Xi} \\ Z_{N\alpha}\tau_{\alpha}^{\Xi N} & 0 & Z_{N\alpha}\tau_{\alpha}^{\Xi N} & Z_{N\Xi}\tau_{\Xi}^{\alpha N} & 0 \end{pmatrix} \times \begin{pmatrix} X_{\alpha\alpha} \\ X_{\Lambda\alpha} \\ Y_{\alpha\alpha} \\ Y_{\Xi\alpha} \\ Y_{N\alpha} \end{pmatrix}, \quad (33)$$

where the Y give the transition amplitude from the initial $(\Lambda\Lambda)\alpha$ state to a final state of the $\Xi N\alpha$, *e.g.* $Y_{\Xi\alpha}$ is the amplitude for $(N\alpha)\Xi \leftarrow (\Lambda\Lambda)\alpha$. In the $\Xi N\alpha$ channel we have three distinguishable particles, and as a result, there are three Y amplitudes, and no antisymmetry is required.

To obtain a better understanding of the structure of these coupled integral equations as well as how the $\Lambda\Lambda$ - ΞN coupling is introduced, we have written the kernel of the above coupled integral equations in the form of a product of the Born terms \mathbf{Z} which is diagonal in the $\Lambda\Lambda\alpha$ - $\Xi N\alpha$ channels, and a quasi-particle propagator $\boldsymbol{\tau}$ that has the coupling between the $\Lambda\Lambda$ and the ΞN channels, *i.e.* $\mathbf{K} = \mathbf{Z} \times \boldsymbol{\tau}$, where

$$\mathbf{Z} = \begin{pmatrix} 0 & Z_{\alpha\Lambda} & 0 & 0 & 0 \\ Z_{\Lambda\alpha} & Z_{\Lambda\Lambda} & 0 & 0 & 0 \\ 0 & 0 & 0 & Z_{\alpha\Xi} & Z_{\alpha N} \\ 0 & 0 & Z_{\Xi\alpha} & 0 & Z_{\Xi N} \\ 0 & 0 & Z_{N\alpha} & Z_{N\Xi} & 0 \end{pmatrix} \quad (34)$$

and

$$\boldsymbol{\tau} = \begin{pmatrix} \tau_{\alpha}^{\Lambda\Lambda} & 0 & \tau_{\alpha}^{\Lambda\Xi} & 0 & 0 \\ 0 & \tau_{\Lambda}^{\alpha\Lambda} & 0 & 0 & 0 \\ \tau_{\alpha}^{\Xi\Lambda} & 0 & \tau_{\alpha}^{\Xi N} & 0 & 0 \\ 0 & 0 & 0 & \tau_{\Xi}^{\alpha N} & 0 \\ 0 & 0 & 0 & 0 & \tau_{N}^{\alpha\Xi} \end{pmatrix}. \quad (35)$$

If we now set the coupling between the $\Lambda\Lambda$ and ΞN channels to zero, *i.e.*, $\tau_{\alpha}^{\Lambda\Xi} = \tau_{\alpha}^{\Xi\Lambda} = 0$, then the three-body matrix integral equation decouples into two sets of coupled equations for the $\Lambda\Lambda\alpha$ and $\Xi N\alpha$ Hilbert spaces, respectively, with the former set of equations being just Eq. (31). The proper inclusion of the different thresholds, associated with the mass difference between the $\Lambda\Lambda$ and ΞN two-body systems, is accounted for by measuring all two-body energies with respect to the $\Lambda\Lambda$ threshold and all three-body energies with respect to the $\Lambda\Lambda\alpha$ threshold. That is, the energy available to the ΞN two-body and $\Xi N\alpha$ three-body channels is $E - \delta_m$, where $\delta_m = m_{\Xi} + m_N - 2m_{\Lambda}$; we understand E to be the appropriate total two-body or three-body energy.

IV. RESULTS AND DISCUSSION

Solution of the equations for the ground state of ${}_{\Lambda\Lambda}^6\text{He}$ was obtained by converting the above integrals equations into a set of coupled linear algebraic equations by replacing the integral with a Gauss-Legendre quadrature rule. For the bound-state problem, the kernel is smooth and well behaved, with no singularities on the real momentum axis. By setting $\tau_{\alpha}^{\Lambda\Xi} = 0$, we can decouple the $\Lambda\Lambda\alpha$ and $\Xi N\alpha$ systems. In turning off the coupling in this way, the $\Lambda\Lambda$ interaction included in the calculation of the binding energy of ${}_{\Lambda\Lambda}^6\text{He}$ is the $\Lambda\Lambda$ diagonal component of the $\Lambda\Lambda$ - ΞN T -matrix from the solution of the coupled-channel problem. When coupling is included, we also include both s - and p -wave $N\alpha$ interactions since both the $P_{\frac{1}{2}}$ and $P_{\frac{3}{2}}$ channels support $N\alpha$ resonances. All other potentials (*i.e.*, $\Lambda\Lambda$ - ΞN , $\Lambda\alpha$ and $\Xi\alpha$) are treated in s -wave only, as this is expected to be the dominant component of these interactions. In Table X we list all three-body channels for the $J^{\pi} = 0^{+}$, $T = 0$ configuration.

We have argued above that only the $\Lambda\Lambda$ component of the full $\Lambda\Lambda$ - ΞN force is responsible for the binding of the hypernucleus, ${}_{\Lambda\Lambda}^6\text{He}$. That is, we suggest the $\Lambda\Lambda \rightarrow \Xi N$ transition is Pauli blocked and, as a consequence, only the $\Lambda\Lambda\alpha$ part of the Hilbert space is necessary to bind the hypernucleus. In Table XI we summarize results for $B_{\Lambda\Lambda}$ for each of the four potentials SA, SB, SC1 and SC2. In each case we consider two different possibilities for the $\Lambda\alpha$ interaction (SYNG and SIsl). Although the $\Lambda\alpha$ interaction is uncertain, (the binding energy of ${}^5_{\Lambda}\text{He}$ being the only experimental data to constrain the interaction) the sensitivity of $B_{\Lambda\Lambda}$ to the type of $\Lambda\alpha$ potential used is minor and does not prevent our being able to discriminate among the types of $\Lambda\Lambda$ - ΞN interaction considered. As the results in Table XI demonstrate, the potentials that support two-body bound states (*i.e.*, SC1 and SC2), overbind ${}_{\Lambda\Lambda}^6\text{He}$, even when only the $\Lambda\Lambda$ component of the force is included. Potential SC1, in which the $\Lambda\Lambda$ system is bound by only ~ 0.7 MeV, predicts a value for $B_{\Lambda\Lambda}$ that is well above the experimental uncertainty associated with $B_{\Lambda\Lambda} = 10.9 \pm 0.6$ MeV. As we increase the strength of the $\Lambda\Lambda$ - ΞN interaction to that of model SC2 (having a bound state of ~ 4.7 MeV), the value of $B_{\Lambda\Lambda}$ increases as expected, severely over binding the hypernucleus. Based on these observations, we conclude that, if the experimental value of $B_{\Lambda\Lambda}$ is to be believed, then the $\Lambda\Lambda$ - ΞN system cannot support a bound state (of at least 0.7 MeV) and still be consistent with the $\Lambda\Lambda$ separation energy in ${}_{\Lambda\Lambda}^6\text{He}$. Finally, we note that the results for potential SB come closest to the experimental value.

In order to test our hypothesis that the $\Lambda\Lambda \leftrightarrow \Xi N$ conversion is suppressed in ${}_{\Lambda\Lambda}^6\text{He}$, we performed bound-state calculations including this coupling term explicitly (*i.e.*, $\tau_{\alpha}^{\Lambda\Xi} \neq 0$). As we have previously suggested, we believe this conversion to be Pauli blocked, because the nucleon involved in the conversion cannot occupy the $1s$ state in a simple shell model picture. For conversion to take place, either a nucleon in the core nucleus must be promoted into a positive parity excited state, or the converted nucleon must go into the $2s$ state. Both configurations require $2\hbar\omega$ in energy and, as a result, are suppressed. To model this many-body effect within the two-body context of an α -particle and a nucleon, we have parameterized the $S_{\frac{1}{2}}$ $N\alpha$ interaction as repulsive. Along with the $N\alpha$ $S_{\frac{1}{2}}$ interaction, we also include the attractive $N\alpha$ interactions in both the $P_{\frac{1}{2}}$ and $P_{\frac{3}{2}}$ channels, because both two-body interactions support resonances, and are coupled to the channel with the $N\alpha$ $S_{\frac{1}{2}}$ interaction. The results of these calculations are collected in Table XII, for various $\Lambda\Lambda$ - ΞN

and $\Lambda\alpha$ interactions. For the $N\alpha$ interactions we use model A of Ref. [55], while for the $\Xi\alpha$ potential we utilize the interaction which we constructed for the Ξ -nucleus system (where the nucleus is ${}^4\text{He}$).

For each of the $\Lambda\Lambda$ - ΞN interactions SA, SB, SC1 and SC2 there is a small increase in the binding energy $B_{\Lambda\Lambda}$, compared with those values listed in Table XI, and essentially independent of the type of $\Lambda\alpha$ interaction considered. This is not surprising, given that we have treated the α particle as an elementary object. The incorporation of the ‘‘Pauli principle’’ for the $N\alpha$ $S_{\frac{1}{2}}$ interaction is not as obvious as it is in the shell-model. However, the increase in $B_{\Lambda\Lambda}$ (0.23, 0.66, 1.38, and 2.36 MeV for potentials SA, SB, SC1, and SC2) is not as large as one might expect to see if the $\Lambda\Lambda \leftrightarrow \Xi N$ coupling was strong in the ${}^6_{\Lambda\Lambda}\text{He}$ hypernucleus. It is evident from comparing results of Tables XI and XII that indeed the coupling is strongly suppressed, in contrast to that in the two-body interactions in free space. The inclusion of a repulsive $N\alpha$ $S_{\frac{1}{2}}$ interaction acts to prevent the $\Xi N\alpha$ part of the Hilbert space from adding much attraction to the three-body system. Furthermore, we must conclude that the coupling between the three-body channels, $\Xi - (N\alpha)_{S_{\frac{1}{2}}}$ in an $\mathcal{L} = 0$ state, and $\Xi - (N\alpha)_{P_{\frac{1}{2}}, P_{\frac{3}{2}}}$ in $\mathcal{L} = 1$ states, is small; this is a result of the three-body dynamics. Because the p-wave $N\alpha$ interactions are strong, we would expect them to provide significant additional attraction if these three-body channels were strongly coupled.

To emphasize our point, we have constructed effective single-channel $\Lambda\Lambda$ interactions designed to reproduce the scattering length $a_{\Lambda\Lambda}$ and effective range $r_{\Lambda\Lambda}$ for all four coupled-channel interactions. The parameters for these potentials SCSA, SCSB, SCSC1 and SCSC2, are listed in Table XIII. Comparing the values of $C_{\Lambda\Lambda}$ with those of the coupled channel potential given in Table IV already gives an indication that the effective potentials are considerably stronger in the $\Lambda\Lambda$ channel. The binding energy of ${}^6_{\Lambda\Lambda}\text{He}$ for the four effective potentials is given in Table XIV, and are all much larger than those shown in Table XI, except for the weakly attractive potential SA. For potential SCSB the increase in binding due to this effective $\Lambda\Lambda$ interaction (compared with potential SB) is ~ 2.5 MeV. This is to be compared with an increase of ~ 0.7 MeV when including the $\Lambda\Lambda$ - ΞN coupling. This difference reflects the extra binding a free space $\Lambda\Lambda$ interaction would give for $B_{\Lambda\Lambda}$.

Others have included repulsive dispersive three-body forces, along with two-body forces, to eliminate such overbinding in Λ hypernuclei. In particular Bodmer *et al.* [32,39,67,68] have included dispersive ΛNN three-body forces. They found it necessary to include repulsive three-body forces to avoid overbinding for ${}^5_{\Lambda}\text{He}$. However, if the effects of the suppression of the ΛN - ΣN coupling are included explicitly, then one can account for the experimental value of $B_{\Lambda}({}^5_{\Lambda}\text{He})$ using a reasonable model of the ΛN - ΣN interaction [49], without the need to introduce significant three-body force effects. Indeed, we find for ${}^6_{\Lambda\Lambda}\text{He}$ that we can account for the binding energy within a realistic model of the $\Lambda\Lambda$ - ΞN interaction (one comparable in strength to that of the nn interaction) without the need to include $\Lambda\Lambda N$ three-body forces. That is, we have shown that incorporation of important two-body effects (inclusion of $\Lambda\Lambda$ - ΞN coupling in the two-body, and the resultant Pauli blocking in the $A = 6$ hypernucleus) can reduce the value of $B_{\Lambda\Lambda}$ to lie within acceptable limits of the available experimental datum.

V. SUMMARY AND CONCLUSIONS

Based upon the information contained in Tables XI and XII in particular, we conclude that it is primarily the $\Lambda\Lambda$ component of the $\Lambda\Lambda$ - ΞN force that is sampled in the ${}_{\Lambda\Lambda}^6\text{He}$ hypernucleus. Furthermore, we observe that potentials SC1 and SC2 are unlikely to be realistic models for the interaction if we are to believe the experimental value for $B_{\Lambda\Lambda}$. Potential SA, on the other hand, predicts a value for $B_{\Lambda\Lambda}$ that lies ~ 0.8 MeV below the lower limit for the experimental value (for the SYNG model of the $\alpha\Lambda$ interaction). Therefore, it cannot be completely discounted. However, potential SB (the model that gives rise to an anti-bound state similar to that in the nn system), leads to a value for $B_{\Lambda\Lambda}$ that is ~ 0.1 MeV above the upper limit of the experimental value, and is, hence, in reasonable agreement with experiment. This potential yields

$$a_{\Lambda\Lambda} \simeq -21.0 \text{ fm} , \quad (36)$$

which is comparable to the 1S_0 nn scattering length. That is, we find agreement with experiment for a model in which the $\Lambda\Lambda$ - ΞN interaction and the nn interaction have comparable overall strength. We emphasize that it is the full $\Lambda\Lambda$ - ΞN interaction that gives rise to a value of $a_{\Lambda\Lambda} \simeq -21.0$ fm. Even though in free space the SB model predicts such a value for $a_{\Lambda\Lambda}$, it can still give a value of

$$-\langle V_{\Lambda\Lambda} \rangle \simeq 4.7 \text{ MeV} \quad (37)$$

in good agreement with the ${}_{\Lambda\Lambda}^6\text{He}$ datum. This value for $-\langle V_{\Lambda\Lambda} \rangle$ is significantly smaller than a similar nn interaction quantity of

$$-\langle V_{nn} \rangle \simeq 6 - 7 \text{ MeV} . \quad (38)$$

It is the suppression of the $\Lambda\Lambda \leftrightarrow \Xi N$ coupling that is responsible for the reduction in $-\langle V_{\Lambda\Lambda} \rangle$ compared with $-\langle V_{nn} \rangle$. In other words, there can exist a $\Lambda\Lambda$ - ΞN interaction that is consistent with the experimental data for $B_{\Lambda\Lambda}$, and at the same time allows for a free space value for $a_{\Lambda\Lambda}$ which is comparable to a_{nn} .

ACKNOWLEDGMENTS

The authors would like to dedicate the present work to the memory of Carl Dover who played a central role in initiating this investigation and in particular the construction of the OBE potential in the strangeness -2 sector. The work of SBC and IRA was supported by the Australian Research Council. That of BFG was performed under the auspices of the U. S. Department of Energy.

APPENDIX A: THE OBE POTENTIAL

In this Appendix we outline the one boson exchange potential in the $S = -2$ sector. Since we have restricted the analysis to s -wave only, the potential has the form given in Eq. (6) with the central and spin-dependent components of the form

$$\begin{aligned} V_\xi &= V_\xi^S + V_\xi^{\text{PS}} + V_\xi^{\text{V}} \quad \xi = c, \sigma \\ &= \sum_i V_\xi^{(i)} \phi(x_i) , \end{aligned} \quad (\text{A1})$$

where the i sum runs over all possible exchanged mesons. The Nijmegen potential D [14] includes the complete nonets of pseudoscalar (PS) $[\pi, \eta, \eta', K]$ and vector (V) $[\rho, \omega, \phi, K^*]$ mesons as well as the exchange of the unitary singlet scalar ϵ meson. The function $\phi(x_i)$ is the standard Yukawa function including the soft cutoff, *i.e.*

$$\phi(x_i) = \left[\frac{e^{-x_i}}{x_i} - \mathcal{C} \left(\frac{\mathcal{M}}{m_i} \right) \frac{e^{-\mathcal{M}r}}{\mathcal{M}r} \right] , \quad (\text{A2})$$

where $x_i = m_i r$. The meson masses m_i are given in Table XV and XVI, while the cutoff mass for all meson exchanges is taken to be $\mathcal{M} = 2500$ MeV. The cutoff strengths \mathcal{C} for the different potentials are given in Table I. For the present potential we follow Dover and Gal [63] and introduce average K and K^* masses given by $\bar{m}_K^2 = m_K^2 - (1/2)[(m_\Xi - m_\Lambda)^2 + (m_N - m_\Lambda)^2]$, with a similar expression for $\bar{m}_{K^*}^2$. To give the ρ and ϵ mesons width, the Nijmegen group [14] have introduced two ρ and two ϵ masses and have taken the linear combination of the exchange of the two mesons; *e.g.* for the ϵ we utilize

$$V_\xi^{(\epsilon)} \phi(m_\epsilon r) \rightarrow \beta_1 V_\xi^{\epsilon_1} \phi(m_{\epsilon_1} r) + \beta_2 V_\xi^{\epsilon_2} \phi(m_{\epsilon_2} r) \quad (\text{A3})$$

and make a similar substitution for ρ meson exchange. The values of the β_i and m_i are given in Table XV. To guarantee that the cutoff is always repulsive, we take $\mathcal{C} < 0$ if $V_\xi^{(i)} > 0$.

The one boson exchange potential, presented diagrammatically in Figs. 1 and 2, for the reaction

$$B_1 + B_2 \rightarrow B_3 + B_4 . \quad (\text{A4})$$

takes the form given in Eq. (A1), with the strength $V_c^{(i)}$ for the central part of the potential given by [30]:

$$V_c^{(i)} = 0 \quad \text{for PS exchange} , \quad (\text{A5})$$

$$V_c^{(i)} = -\frac{g_{B_1 B_3}^{(i)} g_{B_2 B_4}^{(i)}}{4\pi} m_i \left(1 - \frac{m_i^2}{8M_1 M_2} \right) \quad \text{for S exchange} , \quad (\text{A6})$$

$$\begin{aligned} V_c^{(i)} &= \frac{g_{B_1 B_3}^{(i)} g_{B_2 B_4}^{(i)}}{4\pi} m_i \left[1 + \left(\frac{f}{g} \right)_{B_1 B_3}^{(i)} \frac{m_i^2}{4M M_1} + \left(\frac{f}{g} \right)_{B_2 B_4}^{(i)} \frac{m_i^2}{4M M_2} \right. \\ &\quad \left. + \left(\frac{f}{g} \right)_{B_1 B_3}^{(i)} \left(\frac{f}{g} \right)_{B_2 B_4}^{(i)} \frac{m_i^4}{16M^2 M_1 M_2} \right] \quad \text{for V exchange} , \end{aligned} \quad (\text{A7})$$

for the exchanged mesons. The spin-dependent part of the potential, $V_\sigma^{(i)}$, is given by [30]:

$$V_\sigma^{(i)} = \frac{g_{B_1 B_3}^{(i)} g_{B_2 B_4}^{(i)}}{4\pi} \frac{m_i^3}{12M_1 M_2} \quad \text{for PS exchange} \quad (\text{A8})$$

$$V_\sigma^{(i)} = 0 \quad \text{for S exchange} \quad (\text{A9})$$

$$V_\sigma^{(i)} = \frac{g_{B_1 B_3}^{(i)} g_{B_2 B_4}^{(i)}}{4\pi} \frac{m_i^3}{6M_1 M_2} \left[1 + \left(\frac{f}{g}\right)_{B_1 B_3}^{(i)} \frac{M_1}{M} + \left(\frac{f}{g}\right)_{B_2 B_4}^{(i)} \frac{M_2}{M} \right. \\ \left. + \left(\frac{f}{g}\right)_{B_1 B_3}^{(i)} \left(\frac{f}{g}\right)_{B_2 B_4}^{(i)} \frac{M_1 M_2}{M^2} \left(1 + \frac{m_i^2}{8M_1 M_2} \right) \right] \quad \text{for V exchange} . \quad (\text{A10})$$

In Eqs. (A9) and (A10) the coupling constants $g_{B_1 B_3}^{(i)}$ and $f_{B_1 B_3}^{(i)}$ are the electric and magnetic couplings of meson i to baryons 1 and 3, m_i is the mass of the exchanged meson, $M_1 = (M_{B_1} M_{B_3})^{\frac{1}{2}}$ and $M_2 = (M_{B_2} M_{B_4})^{\frac{1}{2}}$. Here, M is a scale mass, assumed to be the mass of the nucleon (M_N). The coupling constants that we need for these potentials can be found in Table XVI.

For strange meson exchange, the potential has the same basic form as $V_{\text{OBE}}(r)$ (*i.e.* Eq. (6)), with the requirement that we replace $\mathbf{t}_1 \cdot \mathbf{t}_2$ with the isospin factor $\sqrt{2}$. That is, formally we have [63]

$$\langle \Lambda\Lambda | \mathbf{t}_1 \cdot \mathbf{t}_2 | \Xi N \rangle_{t=0} = \sqrt{2} , \quad (\text{A11})$$

and introduce space and spin exchange operators, P_x and P_σ respectively. For the 1S_0 state we have $P_x = 1$ and $P_\sigma = -1$.

REFERENCES

- [1] M. Danysz, K. Garbowska, J. Pniewski, T. Pniewski, J. Zakrewski, E. R. Fletcher, *et al.*, Phys. Rev. Lett. **11**, 29 (1963); Nucl. Phys. **49**, 121 (1963).
- [2] D. J. Prowse, Phys. Rev. Lett. **17**, 782 (1966).
- [3] S. Aoki, S. Y. Bahk, K. S. Chung, S. H. Chung, H. Funahashi, C. Hahn, *et al.* Prog. Theo. Phys. **85**, 1287 (1991).
- [4] C. B. Dover, D. J. Millener, A. Gal, and D. H. Davis, Phys. Rev. C **44**, 1905 (1991).
- [5] D. H. Wilkinson, S. J. St. Lorant, D. K. Robinson, and S. Lokanathan, Phys. Rev. Lett. **3**, 397 (1959).
- [6] W. H. Barkas, M. A. Dyer, and H. H. Heckman, Phys. Rev. Lett. **11**, 429 (1963).
- [7] B. Bhowmik, Nuovo Cimento **29**, 1 (1963).
- [8] A. Bechdolf, G. Baumann, J. P. Gerber, and P. Cüer, Phys. Lett. B **26**, 174 (1968).
- [9] J. Catala, F. Senet, A. F. Tejerina, and E. Villar, in *Proceedings of the International Conference on Hypernuclear Physics*, Vol. 2, ed. by A. R. Bodmer and L. G. Hyman (Argonne 1969) p. 758.
- [10] A. S. Mondal, A. K. Basak, M. M. Kasim, and A. Husain, Nuovo Cimento A **54**, 333 (1979).
- [11] See W. Tornow, H. Witala, and R. T. Braun, Few-Body Systems **21**, 97 (1996) and the references cited therein.
- [12] R. H. Dalitz, D. H. Davis, P. H. Fowler, A. Montwill, J. Pniewski, and J. A. Zakrewski, Proc. Roy. Soc. London **A426**, 1 (1989).
- [13] J. J. de Swart, M. M. Nagels, T. A. Rijken, and P. A. Verhoeven, *Springer Tracts in Modern Physics* **60**, 138 (1971).
- [14] M. M. Nagels, T. A. Rijken, and J. J. de Swart, Phys. Rev. D **15**, 2547 (1977).
- [15] M. M. Nagels, T. A. Rijken, and J. J. de Swart, Phys. Rev. D **20**, 1633 (1979); M. M. Nagels, T. A. Rijken, and J. J. de Swart, Ann. Phys. (NY) **79**, 338 (1973).
- [16] P. M. M. Maessen, T. A. Rijken and J. J. de Swart, Phys. Rev. C **40**, 2226 (1989).
- [17] J. J. de Swart, Proceedings of the *U. S. – Japan Seminar on the Hyperon-Nucleon Interaction*, ed. by B. F. Gibson, P. D. Barnes, and K. Nakai, (World Scientific, Singapore, 1994), pp. 37-54.
- [18] R. Timmermans, Proceedings of the *U. S. – Japan Seminar on the Hyperon-Nucleon Interaction*, ed. by B. F. Gibson, P. D. Barnes, and K. Nakai, (World Scientific, Singapore, 1994), pp. 179-188.
- [19] B. Holzenkamp, K. Holinde, and J. Speth, Nucl. Phys. **A500**, 485 (1989).
- [20] K. Holinde, Nuc. Phys. **A547**, 255c (1992).
- [21] A. G. Reuber, K. Holinde, and J. Speth, Czech. J. Phys. **42**, 1115 (1992).
- [22] A. G. Reuber, Proceedings of the *U. S. – Japan Seminar on the Hyperon-Nucleon Interaction*, ed. by B. F. Gibson, P. D. Barnes, and K. Nakai, (World Scientific, Singapore, 1994), pp. 159-168.
- [23] M. Juric, G. Bohm, J. Klabuhn, U. Kreckler, F. Wysotzki, G. Coremans-Bertand, J. Sacton, G. Wilquet, T. Cantrell, F. Esmael, A. Montwill, D. H. Davis, *et al.* Nucl. Phys. **B52**, 1 (1973).
- [24] D. H. Davis and J. Sacton, in *High Energy Physics*, Vol. II, (Academic Press, New York, 1967) p. 365.
- [25] D. H. Davis, Proceedings of the *LAMPF Workshop on (π, K) Physics*, A. I. P. Conf.

- Proc. **224**, ed. by B. F. Gibson, W. R. Gibbs, and M. B. Johnson, (American Institute of Physics, New York, 1991), pp. 38-48.
- [26] A. Bamberger, M. A. Faessler, U. Lynn, H. Piekartz, J. Piekartz, J. Pniewski, B. Povh, H. G. Ritter, and V. Soergel, Nucl. Phys. **B60**, 1 (1973).
- [27] M. Bejidian, E. Descroix, J. Grossiord, A. Guichard, M. Gusakov, M. Jacquin, M. Kudla, H. Piekartz, J. Piekartz, J. Pizzi, and J. Pniewski, Phys. Lett. B **83**, 252 (1979).
- [28] C. B. Dover and H. Feshbach, Ann. Phys. (N.Y.) **198**, 321 (1990).
- [29] C. B. Dover and H. Feshbach, Ann. Phys. (N.Y.) **217**, 51 (1992).
- [30] C. B. Dover (*private communication*).
- [31] B. F. Gibson, A. Goldberg, and M. S. Weiss, Phys. Rev. **181**, 1486 (1969).
- [32] A. R. Bodmer, Q. N. Usmani, and J. A. Carlson, Nucl. Phys. **A422**, 510 (1984).
- [33] H. Bandō, Prog. Theor. Phys. **67**, 669 (1982).
- [34] A. R. Bodmer, Phys. Rev. **141**, 1387 (1966).
- [35] R. C. Herndon, Y. C. Tang, Phys. Rev. **153**, 1091 (1967); **159**, 853 (1967); **165**, 1093 (1969); R. H. Dalitz, R. C. Herndon, and Y. C. Tang, Nucl. Phys. **B47**, 109 (1972).
- [36] B. F. Gibson, A. Goldberg, and M. S. Weiss, Phys. Rev. C **6**, 741 (1972).
- [37] B. F. Gibson, A. Goldberg, and M. S. Weiss, in *Few Particle Problems in Nuclear Interactions*, (North Holland, Amsterdam, 1972), p. 188.
- [38] A. Gal, Adv. Nucl. Physics **8**, 1 (1975).
- [39] A. R. Bodmer and Q. N. Usmani, Nucl. Phys. **A477**, 621 (1988); Phys. Rev. C **31**, 1400 (1985); A. R. Bodmer, Q. N. Usmani, and J. A. Carlson, Phys. Rev. C **29**, 684 (1984).
- [40] J. A. Carlson, Proceedings of the *LAMPF Workshop on (π, K) Physics*, A. I. P. Conf. Proc. **224**, ed. by B. F. Gibson, W. R. Gibbs, and M. B. Johnson, (American Institute of Physics, New York, 1991), pp. 198 - 210.
- [41] K. S. Myint and Y. Akaishi, Prog. Theo. Phys. Suppl. **117**, 251 (1994).
- [42] M. Oka and K. Yazaki, Phys. Lett. **B90**, 41 (1980); M. Oka and K. Yazaki, Prog. Theor. Phys. **B66**, 556 (1981); 572 (1981).
- [43] A. Faessler, F. Fernandez, G. Lübeck and K. Shimuzu, Phys. Lett. **B112**, 201 (1982); Nucl. Phys. **A402**, 555 (1983).
- [44] M. Oka and K. Yazaki, *Quarks and Nuclei*, ed. W. Weise (World Scientific, Singapore, 1984), p. 489.
- [45] M. Oka, *Dibaryons in the Quark Model*, Talk presented at the 10th International Symposium (YAMADA conference XXXV) on High Energy Spin Physics, 1993.
- [46] Y. Koike, K. Shimizu and K. Yazaki, Nucl. Phys. **A513**, 653 (1990).
- [47] M. Oka, K. Shimizu and K. Yazaki, Nucl. Phys. **A464**, 700 (1987).
- [48] C. B. Dover and A. Gal, Prog. in Part. and Nucl. Phys. **12**, 171 (1984).
- [49] B. F. Gibson, I. R. Afnan, J. A. Carlson and D. R. Lehmann, Prog. Theor. Phys. Suppl. No. 117, 339 (1994).
- [50] R. V. Reid, Jr., Ann. Phys. (N.Y.) **50**, 411 (1968).
- [51] I. R. Afnan and B. F. Gibson, Phys. Rev. C **47**, 1000 (1993).
- [52] Y. Yamaguchi, Phys. Rev. **95**, 1628 (1954).
- [53] D. R. Lehman, M. Rai and A. Ghovanlou, Phys. Rev. C **17**, 744 (1978).
- [54] A. Ghovanlou and D. R. Lehman, Phys. Rev. C **9**, 1730 (1974).
- [55] A. Eskandarian and I. R. Afnan, Phys. Rev. C **46**, 2344 (1992).
- [56] Carl B. Dover, *Proceedings of the U.S.-Japan Seminar on the Hyperon-Nucleon Inter-*

- action*, ed. by B. F. Gibson, P. D. Barnes, and K. Nakai (World Scientific, Singapore, 1994), pp. 1-16.
- [57] K. A. Brueckner, C. A. Levinson and H. M. Mahmoud, *Phys. Rev.* **95**, 217 (1954).
 - [58] J. Goldstone, *Proc. Roy. Soc. London* **A239**, 267 (1957).
 - [59] B. D. Day, *Rev. Mod. Phys.* **39**, 719 (1967).
 - [60] Y. Yamamoto and H. Bandō, *Prog. Theor. Phys.* **73**, 905 (1985).
 - [61] Y. Kurihara, Y. Akaishi and H. Tanaka, *Phys. Rev. C* **31**, 971 (1985).
 - [62] A. S. Mondal *et al.*, *Nuovo Cim.* **29**, 1 (1963).
 - [63] C. B. Dover and A. Gal, *Ann. Phys. (N.Y.)* **146**, 309 (1983).
 - [64] E. O. Alt, P. Grassberger and W. Sandhas, *Nucl. Phys.* **B2**, 167 (1967).
 - [65] I. R. Afnan and B. F. Gibson, *Phys. Rev. C* **40**, R7 (1989); **41**, 2787 (1990).
 - [66] I. R. Afnan and A. W. Thomas, *Phys. Rev. C* **10**, 109 (1974).
 - [67] A. R. Bodmer and Q. N. Usmani, *Nucl. Phys.* **A468**, 653 (1987).
 - [68] A. A. Usmani, *Phys. Rev. C* **52**, 1773 (1995).

FIGURES

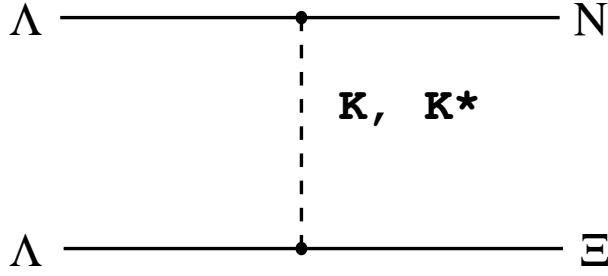


Fig. 1. The first order meson exchange diagram for the $\Lambda\Lambda \rightarrow \Xi N$ process.

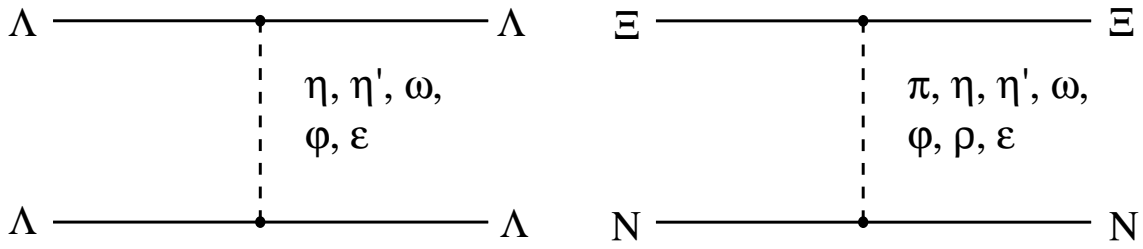


Fig. 2. The first order meson exchange diagrams for the $\Lambda\Lambda$ and ΞN systems.

TABLES

TABLE I. The cutoff parameter \mathcal{C} for the four $\Lambda\Lambda$ - ΞN coupled-channels potentials and the ΞN single-channel potentials specified.

Pot.	\mathcal{C}	Channel	\mathcal{C}
A	157.0	1S_0 t=1	28.65
B	87.0	3S_1 t=0	6.70
C1	66.0	3S_1 t=1	10.9
C2	50.2		

TABLE II. The effective range parameters for the $\Lambda\Lambda$ - ΞN coupled-channels potentials in the 1S_0 partial wave.

Pot.	$a_{\Lambda\Lambda}$ (fm)	$r_{\Lambda\Lambda}$ (fm)	$a_{\Xi N}$ (fm)	$r_{\Xi N}$ (fm)	B.E. (MeV)
A	-1.91	3.36	-2.12-0.75i	3.45-0.45i	UB
B	-21.1	1.86	-2.05-6.53i	2.12-0.21i	UB
C1	7.82	1.41	3.08-5.26i	1.74-0.144i	0.71
C2	3.37	1.0	3.37-2.54i	1.44-0.10i	4.74

TABLE III. The effective range parameters for the ΞN potentials in the various channels.

channel	$a_{\Xi N}$ (fm)	$r_{\Xi N}$ (fm)
1S_0 t=1	-1.94	3.00
3S_1 t=0	-1.75	3.20
3S_1 t=1	-1.81	3.28

TABLE IV. The parameters of the 1S_0 $\Lambda\Lambda$ - ΞN coupled-channel separable potentials. The β s are in fm^{-1} while the $C_{\alpha\alpha'}$ are in fm^{-2} .

Pot.	$C_{\Lambda\Lambda}$	β_{Λ}	$C_{\Xi\Xi}$	β_{Ξ}	$C_{\Lambda\Xi}$
SA	-0.25874	1.3202	-0.32119	1.3301	0.1820
SB	-0.28005	1.1719	-0.44461	1.2749	0.22015
SC1	-0.88154	1.5834	-2.1590	2.0433	0.57062
SC2	-1.4568	1.7752	-0.85766	1.3789	0.55982

TABLE V. The parameters of the ΞN separable potentials for the given channels. The units are the same as in Table IV.

channel	$C_{\Xi N}$	β_{Ξ}
1S_0 t=1	-0.42588	1.4681
3S_1 t=0	-0.37703	1.4352
3S_1 t=1	-0.34869	1.3969

TABLE VI. The effective range parameters for the $\Lambda\Lambda$ - ΞN coupled-channels separable potentials in the 1S_0 partial wave.

Pot.	$a_{\Lambda\Lambda}$ (fm)	$r_{\Lambda\Lambda}$ (fm)	$a_{\Xi N}$ (fm)	$r_{\Xi N}$ (fm)	B.E. (MeV)
SA	-1.90	3.33	-2.08-0.81i	3.44-0.22i	UB
SB	-21.0	2.54	-2.07-6.52i	2.62-0.15i	UB
SC1	7.84	1.48	3.05-5.28i	1.45+0.074i	0.71
SC2	3.36	1.0	3.35-2.50i	1.83-0.10i	4.73

TABLE VII. The parameters of the ΛN central YNG interaction. The strengths are in MeV.

Range β_i (fm $^{-1}$)		1.5	0.9	0.5
1S_0	a	-13.21	-555.2	2686.0
	b	5.705	408.1	-2137.0
	c	-2.412	-135.5	813.6
3S_1	a	-13.57	-389.7	1670.0
	b	5.873	295.7	-1337.0
	c	-1.989	-99.82	519.7

TABLE VIII. The effective range parameters and the binding energy for the $S_{\frac{1}{2}}$ $\Lambda\alpha$ and $S_{\frac{1}{2}}$ $\Xi\alpha$ interactions.

Pot.	a (fm)	r (fm)	B.E. (MeV)
YNG	4.27	2.11	3.1
Isle	4.23	2.10	3.1
DG	4.53	1.98	2.085

TABLE IX. The parameters of the $N\alpha$ separable potentials for the various two-body channels. The β s are in fm^{-1} while the $C_{N\alpha}^\ell$ are in fm^{-2} for the s -wave and fm^{-4} for the p -waves.

Channel	$C_{N\alpha}^\ell$	$\beta_{N\alpha}^\ell$
$S_{\frac{1}{2}}$	1.0519	0.7496
$P_{\frac{1}{2}}$	-1.8221	1.1770
$P_{\frac{3}{2}}$	-7.9735	1.4490

TABLE X. Three-body channels allowed for the $J^\pi = 0^+$, $T = 0$ configuration.

	Channel	t	s	ℓ	j	\mathcal{S}	\mathcal{L}
$\Lambda\Lambda\alpha$:	$\Lambda\alpha(S_{\frac{1}{2}})$	0	$\frac{1}{2}$	0	$\frac{1}{2}$	0	0
	$\Lambda\Lambda(^1S_0)$	0	0	0	0	0	0
$\Xi N\alpha$:	$\Xi N(^1S_0)$	0	0	0	0	0	0
	$N\alpha(S_{\frac{1}{2}})$	$\frac{1}{2}$	$\frac{1}{2}$	0	$\frac{1}{2}$	0	0
	$N\alpha(P_{\frac{1}{2}})$	$\frac{1}{2}$	$\frac{1}{2}$	1	$\frac{1}{2}$	1	1
	$N\alpha(P_{\frac{3}{2}})$	$\frac{1}{2}$	$\frac{1}{2}$	1	$\frac{3}{2}$	1	1
	$\Xi\alpha(S_{\frac{1}{2}})$	$\frac{1}{2}$	$\frac{1}{2}$	0	$\frac{1}{2}$	0	0

TABLE XI. The $\Lambda\Lambda$ separation energy with only the $\Lambda\Lambda$ component of the full interaction included.

Channel	$\Lambda\Lambda$	$\Lambda\alpha S_{\frac{1}{2}}$	$B_{\Lambda\Lambda}$ (MeV)
model	SA	SYNG	9.5078
	SA	SIsle	9.8110
	SB	SYNG	11.606
	SB	SIsle	11.929
	SC1	SYNG	14.533
	SC1	SIsle	14.890
	SC2	SYNG	17.508
	SC2	SIsle	17.889

TABLE XII. The $\Lambda\Lambda$ separation energy for the full $\Lambda\Lambda$ - ΞN interaction.

Channel	$\Lambda\Lambda$ - ΞN	$\Lambda\alpha S_{\frac{1}{2}}$	$N\alpha S_{\frac{1}{2}}$	$N\alpha P_{\frac{1}{2}}$	$N\alpha P_{\frac{3}{2}}$	$\Xi\alpha S_{\frac{1}{2}}$	$B_{\Lambda\Lambda}$ (MeV)
model	SA	SYNG	A	A	A	SDG	9.7381
	SA	SIsle	A	A	A	SDG	10.043
	SB	SYNG	A	A	A	SDG	12.268
	SB	SIsle	A	A	A	SDG	12.594
	SC1	SYNG	A	A	A	SDG	15.912
	SC1	SIsle	A	A	A	SDG	16.268
	SC2	SYNG	A	A	A	SDG	19.836
	SC2	SIsle	A	A	A	SDG	20.507

TABLE XIII. The parameters of the 1S_0 $\Lambda\Lambda$ single channel potentials. The units of β_Λ and $C_{\Lambda\Lambda}$ are the same as in Table IV.

Pot.	$C_{\Lambda\Lambda}$	β_Λ
SCSA	-0.3148	1.3534
SCSB	-0.9995	1.6738
SCSC1	-1.8960	1.9407
SCSC2	-4.7699	2.5310

TABLE XIV. The $\Lambda\Lambda$ separation energy for various single-channel $\Lambda\Lambda$ interactions.

Channel	$\Lambda\Lambda$	$\Lambda\alpha S_{\frac{1}{2}}$	$B_{\Lambda\Lambda}$ (MeV)
Model	SCSA	SYNG	10.007
	SCSA	SIsle	10.317
	SCSB	SYNG	14.138
	SCSB	SIsle	14.494
	SCSC1	SYNG	17.842
	SCSC1	SIsle	18.225
	SCSC2	SYNG	23.342
	SCSC2	SIsle	23.750

TABLE XV. The weighting parameters β_i and the meson masses m_i in MeV used to simulate a width for the ρ and ϵ mesons.

Meson	β_1	m_1	β_2	m_2
ρ	0.15874	628.74	0.78321	878.18
ϵ	0.19986	508.52	0.55241	1043.79

TABLE XVI. Coupling constants $g_{BB'}^{(m)}$ and $f_{BB'}^{(m)}$ for PS, V and S meson exchanges, for Nijmegen model D. Also included are the masses of the exchanged mesons in MeV.

Meson m	Mass	$NN m$	$\Xi\Xi m$	$\Lambda\Lambda m$	$\Lambda\Xi m$	$\Lambda N m$
πg	138.03	3.66	-0.11			
ηg	548.8	2.73	-3.289	-1.361		
$\eta' g$	957.57	3.89	5.015	4.639		
$K g$	457.83				1.986	-4.16
ρg		0.594	0.594			
f		4.817	-1.60			
ϕg	1019.5	-1.124	-2.806	-1.965		
f		-0.51	-5.06	-4.298		
ωg	782.6	3.373	2.184	2.779		
f		2.34	-0.878	-0.338		
$K^* g$	871.63				1.032	-1.032
f					0.934	-4.64
ϵg		5.032	5.032	5.032		